THE MECHANISM OF OXIDATION OF FULLERENES WITH MOLECULAR OXYGEN

M. Wohlers, A. Bauer, Th. Belz,Th. Rühle,Th. Schedel-Niedrig, R. Schlögl
Fritz Haber Institut der Max Planck Gesellschaft
Faradayweg 4-6, D-14195 Berlin, FAX -4930-8413-4401

INTRODUCTION

The novel allotrope of carbon, fullerene is a molecular analogue to the other form of sp^2 hybridised carbon, graphite. In our general attempt to understand the carbon-oxygen reaction at an atomic level we use fullerenes as reference compounds in oxidation studies as they will not exhibit influences of electronic defects on the reactivity. The van der Waals crystals of C_{60} and of C_{70} can be prepared by slow sublimation with single crystalline quality and in absence of any detectable phase impurity due to the molecular separation procedures for the sublimation precursors. It is equally convenient to work on thin films of fullerenes on e.g. silicon (100) surfaces, on large single crystals and on sublimed powder.

Solid fullerenes are air-sensitive materials. They degrade quickly within minutes into a stage of reduced solubility and become eventually fully polymerised upon air/sunlight exposure at 300 K[1]. This property is reminiscent on coal degradation, a process in which a variety of gases are released at low rates. We first investigate this initial step of reactivity of fullerenes with air using temperature-programmed methods.

Upon thermal treatment gasification sets in at 573 K with a steep increase in rate at 720 K [2]. We will investigate the steps of oxygen activation and fullerene attack in this window of low reactivity by FT-IR , by X-ray absorption spectroscopy and by XPS.

The pattern of gasification in temperature-programmed TG-MS experiments will be compared for the C_{60} fullerene and several other carbon materials in order to evaluate on the validity of the fullerene oxidation as model for the graphite oxidation reaction.

Intercalation of oxygen into the octahedral voids of C_{60} crystals was found to proceed without oxygen dissociation at 300 K [3]. The process was described as being reversible at 300 K. Polymerisation of C_{60} at 300 K was observed to proceed to 80% in seven days under oxygen containing 2.6 % ozone [4]. Photo-oxidation at 300 K was investigated with a thin film of C_{60}. An intermediate di-carbonyl structure of a fullerene dioxide was suggested based upon an IR absorption at 1750 cm-1. A second broad absorption at 1000 cm-1 remained largely unexplained [5].

High-temperature oxidation of C_{60} was found to begin at 525 K. IR bands at 1780 cm-1 were assigned to cyclic anhydrides, a second feature at 1590 cm-1 to isolated C=C double bonds. Additional discrete peaks at 1102 cm-1, 1037 cm-1 and 958 cm-1 which are superimposed on a broad intense background remained unassigned [6]. The possible presence of the fullerene monoxide as epoxide structure can be ruled out on the basis of the absence of its single intense fingerprint peak at 867 cm-1. The reactivity of fullerenes and graphitic carbons against oxidation in air was studied with kinetic methods [7]. Several batches of C_{60} showed different quantitative reaction behaviour but produced all a mixture of CO and CO_2 in a two-peak reaction profile centred around 730 K. A significant weight uptake in oxygen of 0.73 mole oxygen per mole fullerene was detected at lower temperature than the reaction onset occurred. Intercalation of CO_2 during attempts to determine the surface area was observed whereas dinitrogen did not intercalate. We have previously studied the interaction of oxygen with fullerenes using a variety of methods. The correlation of these data with kinetic observations is described in a recent review paper [8].The present work contains new results which are based upon the observation that the pre-history of the material plays an essential role in its gas-solid interface chemistry. Contrary to the basic expectations, the defect structure of the molecular crystal controls the intercalation of gases into the void system of the crystal and pre-determines the low-temperature reaction to oxygen-adduct precursors and controls the degradation of the molecular crystal by oxidative polymerisation. For this reason, even air-exposure for minutes causes irreversible damage to a fullerene crystal and generates an ill-defined initial status for a reaction experiment. All sample preparation and fullerene manipulation was carried out with freshly sublimed material in a glove box with a controlled level of less than 1.0 ppm of oxygenate contamination. This treatment gave quantitatively reproducible data with no differences in characteristic parameters between sample batches and minimised the weight uptake prior to oxidation. In this way characteristic differences between C_{60} and C_{70} became apparent as the different fullerene structures cause differences in reactivity which are smaller, however, than the spread in properties due to ill-defined materials. The air-induced degradation destroys the molecular nature of the fullerene crystal first before more obvious effects like the accumulation of oxides can be detected spectroscopically.

RESULTS

INTERCALATION OF OXYGEN

Clean fullerenes were transferred in a TDS apparatus and exposed in-situ for 24 h to synthetic air at ambient pressure. The results of the following TDS are shown in Figure 1 for the two fullerenes. The

two experiments first show that both fullerenes can intercalate a large amount of Ar during storage at 300 K. They further intercalate oxygen which replaces partly the Ar during exposure to air at 300 K. Furthermore, the oxygen reacts with the carbon skeleton under formation of labile C-O
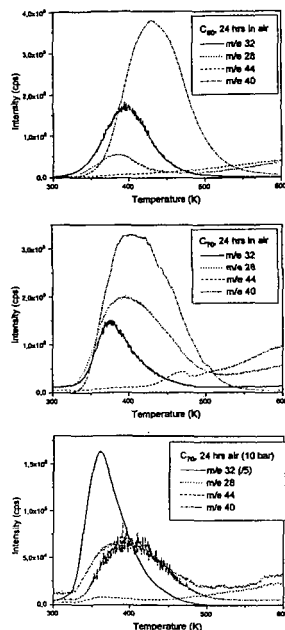

Figure 1. TDS profiles of fullerenes stored under Ar after exposure to air at 300 K and ambient pressure. The linear heating rate was 0.27 K/s. Desorption occurred into UHV. The sample size was with 10 mg identical for both experiments. The experiments were halted at 623 K due to beginning sublimation . The absence of nitrogen under the m/e 28 peak was checked with the absence of an m/e 14 peak. The high pressure experiment (bottom plot) was carried out with a different sample holder and a different sample mass. Note the reduced scale for the m/e 32 peak.

groups or even under formation and intercalation of CO as can be seen from the m/e 28 traces. This reactivity is quite different for the two fullerenes with C_{60} being more stable, as expected from its more „aromatic" and highly symmetric valence electronic structure. Above 450 K both fullerenes react in a thermally activated form with oxygen which was not evolved at 400 K /380 K respectively. This oxygen seems to be present in a more strongly bound and already activated form(epoxide) converting into gasification products at temperatures well below the literature values of gasification activity (2,6,8). The shapes of the desorption profiles indicate different reaction orders caused by the different relevance of bulk diffusion terms on the overall process. The spherical symmetry of C_{60} giving rise to isotropic gas diffusion is more suitable to enclose all gases irrespective of their chemical nature (Ar and di-oxygen), for the uniaxially elongated C_{70} molecule the gas diffusion in its solid is anisotropic but the chemical interaction seems less efficient as evidenced by the lower initial desorption temperature.

The fact that the noble gas desorbs at higher temperatures than the di-oxygen can be accounted for by the different location in the crystal. The oxygen is intercalated in an outer shell of each crystal, the Ar evolves from the inner core. In addition, it has to penetrate the damaged regions of the fullerene crystals which occur as consequence of the partial gasification. As the precursor to the gasification is molecularily disperse, this reaction is not topotactic and attacks every molecule within the shell of intercalation. A large number of partly oxidised molecules with dangling bonds and reactive C=C fragments will remain which can stabilise themselves by polymerisation into a three-dimensional network of non-planar basic structural units. In the presence of oxygen these defective fullerenes are activated precursor structures for enhanced gasification.

Raising the total pressure of air to 10 bars causes the reaction front to move deeper into each crystal This is illustrated for C_{70} where the di-oxygen desorption occurs at the same position but with a much higher intensity than after exposure at one bar. The „noise" on the Ar trace indicates the eruptions of the gas protruding through the now dense solid-solid reaction interface between oxidised and intact fullerene. It is noted that the fraction of di-oxygen which is activated to cause gasification is not changed by the total pressure which only increased the abundance of molecular oxygen intercalated.

In all these experiments the evolution of CO_2 is low but begins exactly with the evolution of di-oxygen. This indicates that only few fullerene molecules are more deeply oxidised than to the carbonyl stage. The fact that in all experiments a rise in the CO_2 partial pressure above 500 K is observed, indicates that a second process of oxidation requiring a higher thermal activation occurs and that a significant amount of oxygen which does not recombine to di-oxygen, resides within the fullerene crystals. It was verified that this sequence of events is independent of the optimised low heating rate.

The observation that C_{60} holds gas molecules more strongly than C_{70} was verified in a static experiment proving the ability of the system to intercalate molecular CO in the same way as molecular oxygen. Ar-loaded fullerenes were degassed with He at 573 K in-situ in a high pressure DRIFTS cell and exposed to 5 bar CO at 400 K for 1h. Both intercalated species show a red shift (2125 cm-1) to the gas phase (2170.21 cm-1) and C_{60} an extra shift of 5% which is in the expected order of magnitude according to the TDS experiments. This experiment is a chemical probe for the overall weak bonding interaction between fullerene host and diatomic guest molecules.

ELECTRONIC STRUCTURE OF OXO-INTERMEDIATES

Photoemission and photoabsorption with tuneable excitation wavelengths were used to study the chemical bonding of the intermediates causing the CO emission at 370-400 K and the enhanced CO_2 emission at 570 K. The valence band electronic structure of both fullerenes is characterised by a sequence of well-resolved molecular states which were probed with 100 eV excitation energy to
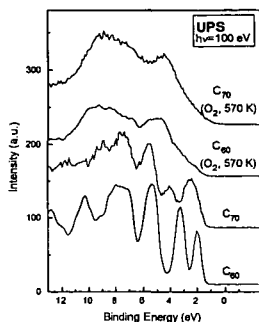
Figure 2: Valence band spectra of fullerene films in their pristine state and after oxidation at 570 K in 500 mbar oxygen (in-situ experiments). The data were recorded at the SX700 1 beamline at the BESSY synchrotron. The Fermi edge was calibrated with a gold sample.

ensure a minimum cross section modulation of σ and π states. This situation is not drastically altered upon intercalation of oxygen at 300 K and heating up to 400 K where already significant chemical reactivity was detected by the bulk-sensitive TDS technique. This implies that the average surface structure is containing up to 400 K still a large abundance of intact fullerene molecules. As can be seen in Figure 2, the surface undergoes complete restructuring upon heating to 570 K and transforms into a polymer structure with extended electronic states characterised by a resonance at 4.6 eV and a broad band around 9.5 eV. These peaks are not those of graphite (2.8 eV and 7.5 eV) but belong to oxygenated (O2p emission at 4.6 eV) partly unsaturated carbon-carbon bond systems. The corresponding C 1s XPS data show three structures at 285. 6 eV for the carbon-carbon skeleton (not graphitic, would be at 284.6 eV) and at 287.1 eV and 289.2 eV for oxygen-carbon single and double bonds. This classifies the chemical reaction leading to CO emission as a process creating mainly defective molecules such as holey fullerene cages with some oxygen functionalities at the empty co-ordination sites. Further thermal treatment is required to remove the C-O functions under CO_2 evolution and to create free carbon co-ordination sites which are saturated by homo-polymerisation with either intact molecules (they act as electrophilic unsaturated entities) or with neighbouring damaged cages. The abundance of oxygen functionalities is larger on C_{70} than on C_{60} although both species give rise to exactly the same spectral positions indicating the close similarity of the chemical bonding.

The modified reactivity of oxygen at different temperatures should be reflected in different chemical bonding of the oxygen precursors which must be present in a more reactive form at 370 K than at 570 K. X-ray absorption spectroscopy is well-suited to prove this as it is element-specific and offers high chemical selectivity. The discrimination of the chemical structure of the oxygen precursors at the two temperatures is shown in Figure 3. At 370 K a species with oxygen single bonds well-compatible with an epoxide (but no peroxide) or an ether structure is detected. The characteristic feature for this is the low intensity of the π* resonance indicating the hybridisation/occupation of these states. At 570 K the oxygen is bonded via double bonds as can be seen from the now prominent π* resonance at 532 eV.
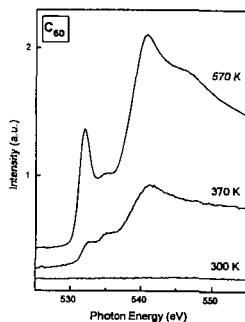
Figure 3: X-ray absorption spectra at the O 1s edge of C_{60} films oxidised at 370 K and 570 K in 500 mbar oxygen for 10 h each. The absence of any detectable oxygen after exposure of the film at 300 K indicates that the chemical bonding of intercalated molecular oxygen was too weak to prevent desorption of the surface-near layers in the UHV of the spectroscopy experiment.

DYNAMICS OF THE OXIDATION

In-situ DRIFTS spectroscopy was used to investigate the participation of the two oxo-intermediates in steady state reaction. The lowest possible temperature at which steady state conversion occurred with both fullerenes was 570 K. At this temperature the samples were exposed to 250 ml/min synthetic air and spectra were recorded as difference spectra to the initial state. In previous experiments it was shown that also at 470 K the formation of additional IR absorptions around 750 cm-1 and 1000 cm-1 occurred which is in agreement with the formation of carbon-oxygen insertion precursor compounds. The data in Figure 4 provide clear evidence for the formation of several oxygen-containing intermediates which are present under steady state oxidation. The low temperature was chosen to allow sufficient data to be accumulated for verification of the steady state. The spectra indicate the same functional groups to be formed than detected in a recent study of oxidised carbon blacks (9). The spectral quality is, however, much better in the present case due to the detection of in-situ spectra (without intermitting the oxidation process and without dilution of the carbon materials).

We observe a split carbonyl band around 1750 cm-1 indicating the presence of other C=O groups besides the cyclic anhydrides for which the high frequency of the absorption is characteristic. The 1580 cm-1 band for isolated double bonds is very prominent and occurs in both fullerenes with the
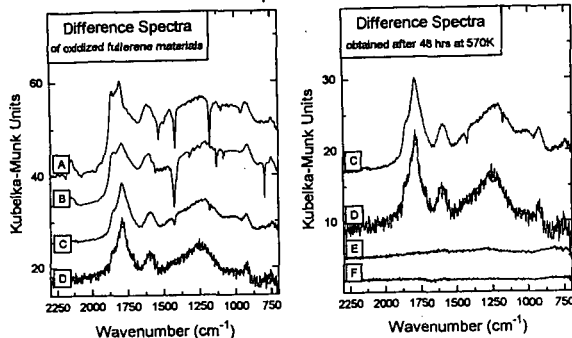
Figure 4: DRIFTS spectra of several fullerene and carbon materials during in-situ oxidation at 570 K. The left panel reports difference spectra after 20 h on stream, the right panel after 48 h oxidation. The burn-off was after 48 h below 10%. Samples were: $A=C_{60}$, $B=C_{70}$, C=fullerene black raw, D= fullerene black after extraction of solubles with toluene, E= activated carbon Norit A, F= graphitic electrode deposit (nanotubes).

same intensity irrespective of the quite different initial electronic structure. The negative sharp bands arise from the loss of molecular fullerene abundance in the gasifying samples. We note that in the non-extracted fullerene black the molecular fullerenes are oxidised preferentially over the other carbon as the bands of C_{60} occur as negative pattern. The molecular bands are superimposed on a broad structure peaking at 1000 cm-1, which was observed in all oxidation studies of fullerenes (6,8) and with oxidised carbon blacks (9). C-O single bond features and the fingerprints of C-C overlap here with high frequency aromatic substitution bands. Such bands occur further at lower frequencies of about 900 cm-1 and 750 cm-1. All these features were also detected in the carbon black oxidation study (9) and are discussed there with respect to the previous literature. The perfect agreement of the spectral features between all materials with nominally only sp^2 bonding clearly reveals that the reaction mechanism detected in detail for the model compounds of fullerenes should qualitatively apply for planar sp^2 carbon materials.

GASIFICATION OF FULLERENES

Temperature-programmed gasification data were obtained from TG-MS experiments in synthetic air (250 ml/min, 5K/min heating ramp). The results for C_{60} are displayed in Figure 5.
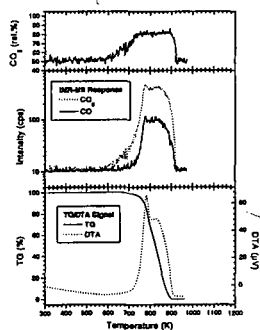

Figure 5: Combined TG-MS gasification experiment of 2.5 mg C_{60} in synthetic air. A horizontal sample pan with a specially directed gas supply and a high throughput ensured the absence of mass transport limitations. A special mass-spectrometer of the IMR-MS type allows to monitor the selectivity without interference with detection of molecular nitrogen and without fragmentation overlap. Note the log ordinate in the MS response plot. The weight uptake before gasification is low due to the high crystal quality of the material which was not air-exposed prior to the gasification experiment.

The gas evolution curve indicates the onset of gasification at 570 K in agreement with the data of Figure 1 (2,6). The selectivity changes in the initial stages of low-temperature oxidation which are dominated by the reaction of precursor compounds. Their abundance is with high-quality crystals so low that the weight uptake of less than 2% between 470 K and 570K is not visible in the overall weight change pattern. Contrary to the reaction pattern for all planar carbon samples which gasified under our experimental conditions all in a double-peak fashion with a slower initial rate and an accelerated second main reaction, the C_{60} fullerene gasifies also in a two-step sequence (7) but with an accelerated initial event. This is taken as indication for the action of the accumulated precursor compounds which leave a large number of defective fullerene molecules after cage-opening oxidation steps. The DTG curve (not shown) reveals that about 20 % of the total mass burns with the accelerated rate. This amount of material coincides with the number of molecules in the skin of oxygen penetration under ambient pressure which was shown to exist in the data of Figure 1.

THE REACTION MECHANISM

The observations indicated above and results from kinetic experiments (2,8) can be combined in a sequence of events for the fullerene oxidation. It is pointed out that no qualitative difference was found for the two molecular fullerenes and the DRIFTS data indicated that the mechanism should also apply for other sp^2 carbon materials. A schematic representation is given in Figure 6, for energetic details see ref. (8).
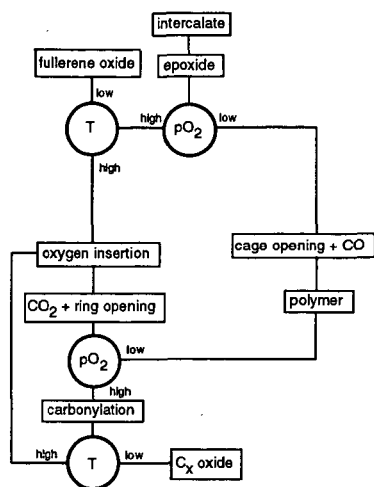
111

Figure 6: Schematic diagram of the sequence of events in fullerene oxidation: The end products besides CO and CO₂ are fullerene oxides, a homopolymer and carbon oxides with defective fullerene structures. The control variables are oxygen partial pressure and temperature.

The reaction starts with an intercalation of molecular oxygen into the van der Waals gaps of the molecular solids. With little thermal activation dissociation occurs and labile epoxides are formed besides activated atomic oxygen which will react with other electrophilic centres on the fullerene molecules. As long as the temperature is kept low (370 K) and the oxygen partial pressure remains present, the epoxides will be retained as fullerene oxides (epoxide or oxygen insertion compound). These materials are, however, not stable and will eventually react under ring opening and CO evolution to a defective fullerene molecule. Stabilisation of this state will occur at low oxygen pressures by homo-polymerisation. At higher partial pressures oxygen will be inserted in the form of e.g. cyclic anhydrides. Above 470 K these structures will evolve CO_2 and cause ring opening in the already attacked fullerene molecule. Should the oxygen partial pressure be low again (e.g. in TDS experiments, or during thermal processing), stabilisation by polymerisation will occur. At still sufficient partial pressures of oxygen carbonylation of the defective structure (5) will follow which remains as metastable product up to 570 K but which gasifies readily at higher temperatures entering a reaction loop ending with complete combustion (6). The reaction product of a polymer will not occur frequently with planar carbons (pinning defect) but the other products as well as the control variables do also occur with conventional carbon materials. The non-planar bonding geometry of the fullerene surface leads to an accumulation of the metastable intermediate products of carbon oxidation as they are formed at lower temperatures than on planar surfaces. For this reason it was possible to observe these intermediates in convenient abundance (9) for spectroscopic characterisation. At higher temperatures of above 700 K where gasification rates become significant for all carbon materials (7) the abundance of the intermediates will be much reduced also for fullerene carbon. Their ease of formation may, however, affect the overall kinetics detectable in macroscopic gasification experiments (7) as illustrated with Figure 5. The relevance of molecular intercalation of oxygen in graphitic carbon and the eventual localisation in between graphene galleries or at defect sites is currently under study. The higher temperatures required for intercalation in graphitic carbon than for fullerene carbon renders any detection with structural methods difficult as can be estimated from the localisation (10) of the extra oxygen in C_{60}.

In conclusion, the different topologies of curved fullerenes and planar sp^2 carbon cause a different abundance of oxo-intermediate compounds at low reaction temperatures. The higher chemical energy of the curved fullerenes allows for a lower activation energy for intermediate formation as well as the total „internal" surface of the fullerene crystal reacts as compared to the low abundance of reactive prismatic surfaces in planar carbon. High quality spectra were accessible for the intermediates allowing to observe some atomistic details of the carbon oxidation process.

ACKNOWLEDGEMENT

REFERENCES

(1) R. Taylor, J.P. Parsons, A.G. Avent, S.P. Rannard, T.J. Dennis, J.P. Hare, H.W. Kroto, D.R.M. Walton, *Nature,* 351, (1991) 277

(2) H. Werner, M. Wohlers, D. Bublak, J. Blöcker, R. Schlögl, *J. Full. Sci. Technol.,* 1, (1993), 457

(3) R.A. Assink, J.E. Schirber, D.A. Loy, B. Morosin, G.A. Carlson, *J.Mater. Res.,*7, (1992), 2136

(4) D. Heyman, L.P.F. Chibante, *Chem. Phys. Lett.,* (1993), 207

(5) C. Taliani, G. Ruani, R. Zamboni, R. Danielli, S. Rossini, V.N. Denisov, V.M. Burlakov, F. Negri, *J. Chem. Soc., Chem. Commun.,* (1993), 220

(6) A.M. Vassallo, L.S.K. Pang, P.A. Cole-Clarke, M.A. Wilson, *J. Am. Chem. Soc.,* 113 (1991), 1103

(7) I.M.K. Ismail, S.L. Rodgers, *Carbon,* 30, (1992), 229

(8) M. Wohlers, A. Bauer, Th. Rühle, F. Neitzel, H. Werner, R. Schlögl, *J. Full. Sci. Technol.,* (1996), in press

(9) P.E. Fanning, M.A. Vannice, *Carbon,*31 , (1993), 721

(10) W. Bensch, H. Werner, H. Bartl, R. Schlögl, *J. Chem. Soc., Faraday Trans.,* 90, (1994), 2791